

High-Cycle Fatigue of IN 713LC

Ludvík Kunz^{1,a}, Petr Lukáš^{1,b}, Rastislav Mintách^{1,c} and Radomila Konečná^{2,d}

¹Institute of Physics of Materials, Academy of Sciences of the Czech Republic, Žitkova 22, 616 62 Brno, Czech Republic

²University of Žilina, Univerzitná 1, 010 26 Žilina, Slovak Republic

^akunz@ipm.cz, ^blukas@ipm.cz, ^cmintach@ipm.cz, ^dradomila.konecna@fstroj.uniza.sk

Keywords: IN 713LC; High-cycle fatigue; Casting defects; Extreme value statistics.

Abstract. High-cycle fatigue strength of Ni-base superalloy IN 713LC was experimentally determined for symmetrical loading and for loading with tensile mean stresses at a temperature of 800 °C in air. An analysis of the influence of microstructure on fatigue crack initiation and related fatigue strength was performed. Statistical method of the largest extreme value has been applied to characterize the casting defect distribution.

Introduction

Nickel-base cast superalloy IN 713LC belongs to the first generation of the polycrystalline cast materials with nearly equiaxed grains. It is a low carbon variant of IN 713 alloy, which has been used since 1950 for low pressure blades and vanes. Conventionally cast superalloys were developed to reach superior creep properties required by turbine industry. The fatigue properties were believed to be less germane to reliability of turbines. The up to now research attention was paid mainly to the low-cycle fatigue life, e.g. [1], and to the thermomechanical fatigue behavior, because they are closely related to start up and shut down of engines [2]. The dislocation structure development, strain localization and low-cycle fatigue (LCF) behavior have been studied in detail [3]. The high-cycle fatigue (HCF) properties were considered to be less prominent and therefore the HCF data related to superalloys are not readily found in literature even for often used engineering superalloys. Though IN 713LC is an old engineering material, it has been expanding in the European gas turbine industry in the recent years. In order to develop new prediction methods the generation of high quality material test data is necessary [4].

The high temperature mechanical performance of IN 713 depends critically on microstructure. It can dramatically vary according to the casting conditions. The problem is that even when nominally the same material and casting conditions are applied, the variations in microstructure of different batches may be substantial and they can result in appreciable differences of mechanical properties. It has been shown long time ago that the fineness of cast microstructure influences the creep behavior in a substantial way [5]. However, similar studies related to the influence of microstructure on fatigue properties are not available, at least in scientific electronic databases and in available open literature.

Polycrystalline cast superalloys are typical by casting porosity. Though it is relatively small in volume, usually below 1%, it can reduce the rupture life and rupture ductility under sustained creep loading and result in large scatter of fatigue life. Hot isostatic pressing technology can be used for closing of porosity but a creep property improvement was reported to be variable. Generally, the scatterband of Larson-Miller parametric plot of the stress rupture capability is narrower after hot isostatic pressing when compared to the untreated material. Beneficial effect was reported also for S-N curves both in LCF and HCF regions, but no detailed or statistical studies are available [6].

Two decisive fatigue crack initiation types are observed in Ni-base cast superalloys. Fatigue cracks initiate at defects, which are often below the resolution of non-destructive defectoscopy, i.e. on defects existing in “defect free” components from the engineering point of view. Initiated cracks

than propagate non-crystallographically. The second type of fatigue crack initiation is characteristic by development of crystallographic facets, often of large dimensions. There is no well explained and understood relation of this crystallographic type of fatigue crack initiation to the material structure, though it has been reported many years ago that casting defects are often observed at the site of initiation of crystallographic cracks [7].

The object of this paper is to determine the fatigue strength of IN 713LC at 800 °C in HCF region and to analyze the influence of microstructure on fatigue crack initiation and fatigue life. The examination of fatigue strength was performed both for symmetrical loading and for cyclic loading with tensile mean stresses.

Material and experiments

Material for experiments was cast by PBS Velká Bíteš, a. s. company. Three, from the point of view of technology, nominally identical batches denoted as 1, 2 and 3 were used for experimental determination of high-cycle fatigue strength of IN 713LC superalloy. The batches were cast in the company within two years. The grain size determined by means of linear intercept method was 3 ± 0.5 μm . Conventionally cast rods of 20 mm in diameter and 100 mm in length were manufactured by nominally identical casting process. All rods were controlled by conventional x-ray non-destructive defectoscopy and were found “defect free”, which means that the defect size was below the resolution limit of the method, which is about 0.5 mm.

Cylindrical button-end specimens of 5 or 6 mm in diameter and with 35 mm long gauge length were machined from the cast semiproducts. The final operation of specimen machining was fine grinding.

Fatigue testing was performed in HCF region by means of two 100 kN resonant testing systems operating under controlled load. The mean stress has been controlled since the start of heating. It was kept at zero level as long as the specimen was not at the desired temperature for at least two hours. Then the chosen non-zero mean stress was set up during several seconds. After that the resonant system was switched on. The full chosen stress amplitude was reached during several hundreds of loading cycles. The frequency of loading was either 105 ± 3 or 110 ± 3 Hz according to the applied resonant fatigue machine. The heating was performed in an electric furnace. Tests were run in laboratory air. The long-term stability of temperature of specimen gauge length was within $\pm 1^\circ\text{C}$. The temperature gradient at the central part of the gauge length was smaller than $3^\circ\text{C}/\text{cm}$.

In order to perform statistical evaluation of casting defect distribution in particular batches of IN 713LC, inspection of polished surface on longitudinal axial sections of gauge length of specimens were carried out by means of light microscopy. Image analysis software was used to determine the size of casting defects. The sampling for determination of the largest extreme value distribution was performed on inspection areas $S_0 = 1.827 \text{ mm}^2$. The size of defects was determined in terms of square root area. The largest defect area $\sqrt{\text{area}_{\text{max}}}$ was determined on 25 places chosen on a polished axial section of a part of the specimen gauge length of 5 x 20 mm dimension. The results of measurement were processed by the largest extreme value distribution method [8] and presented in terms of Gumbel plots.

Results

The experimentally determined S-N data in HCF region for the stress symmetrical loading at temperature of 800 °C can be seen in Fig. 1 in a semi-logarithmic plot. They exhibit very large scatter. The differences in the lifetime of particular specimens at the same stress level are most pronounced in the region where some of specimens had lifetime higher than 10^7 cycles. For example, at the stress amplitude $\sigma_a = 170 \text{ MPa}$ the specimen No. 89 (indicated in the Fig. 1) had the fatigue lifetime 1.19×10^5 cycles, whereas another specimens from the same batch had the lifetime

higher than 10^7 cycles. This represents scatter in the range more than two and half orders of magnitude. Large scatter of S-N data indicates strong influence of defects. Run-out specimens

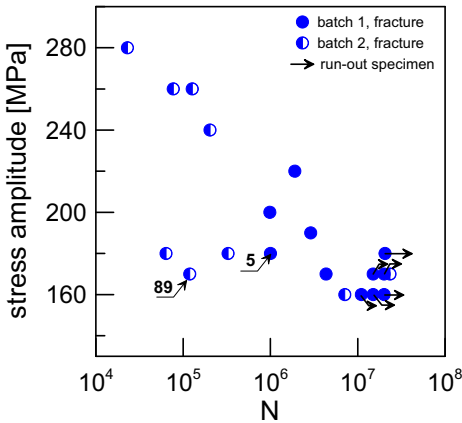


Fig. 1 Fatigue life of IN 713LC at 800 °C in air. Symmetrical loading.

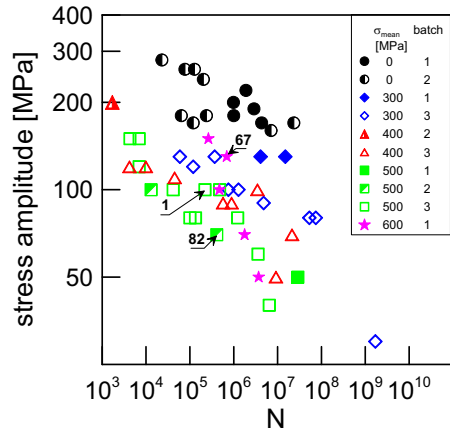


Fig. 2 Comparison of S-N data of IN 713LC at 800 °C in air for symmetrical loading and loading with tensile mean stresses.

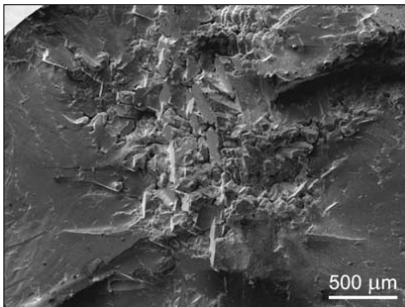


Fig. 3 Casting defect in the site of fatigue crack initiation.

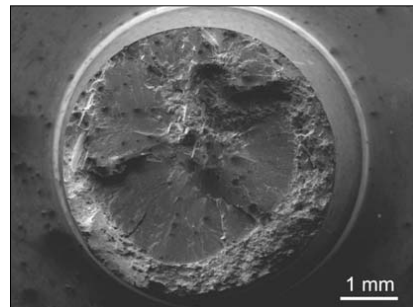


Fig. 4 Fatigue fracture surface with internal crack initiation.

with fatigue life higher than 10^7 cycles together with broken specimens can be found in the σ_a interval from 160 to 180 MPa. Above 180 MPa all tested specimens failed. Full and half-full points in Fig. 1 mark results obtained on specimens manufactured from two nominally identical batches. No run-out points correspond to the material from the batch 2. This indicates substantially worse high-cycle fatigue performance of this batch.

The experimental results for loading with tensile mean stresses $\sigma_{mean} = 300, 400, 500$ and 600 MPa are shown in Fig. 2 in log-log plot. Data from Fig. 1 corresponding to the symmetrical cycling are shown for comparison. Only data from failed specimens are plotted. Following conclusions can be drawn from the Fig. 2: (i) Tensile mean stress reduces substantially the fatigue strength in the high-cycle fatigue region. (ii) Though there is a considerable scatter of data, differences in the fatigue strength of individual batches can be recognized. For example, for $\sigma_a = 150$ MPa and $\sigma_{mean} = 300$ MPa the full points corresponding to the batch 1 are shifted to higher numbers of cycles to fracture when compared to the open points corresponding to the batch 3. The

same statement can be made from the comparison of fatigue life of specimens from the batch 1 at $\sigma_{\text{mean}} = 600$ MPa and σ_a above 100 MPa and specimens from the batches 2 and 3 loaded even at lower mean stresses.

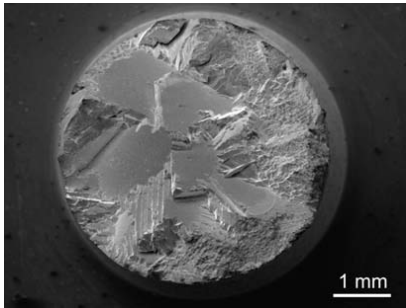


Fig. 5 Crystallographic initiation of fatigue crack.

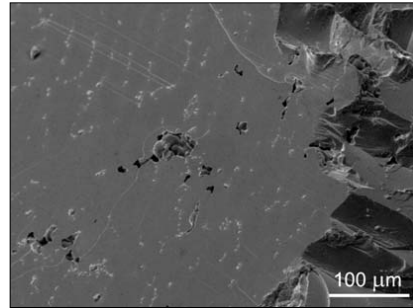


Fig. 6 Crystallographic fracture surface intersecting casting defects.

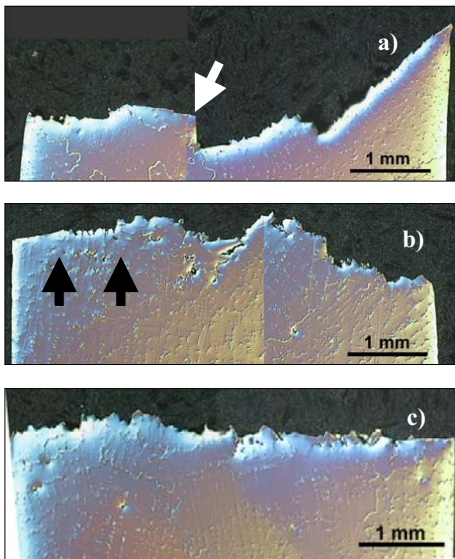


Fig. 7 Fracture profiles of specimens.

- a) $\sigma_{\text{mean}} = 600$ MPa and $\sigma_a = 130$ MPa, batch 1,
- b) $\sigma_{\text{mean}} = 500$ MPa and $\sigma_a = 70$ MPa, batch 2,
- c) $\sigma_{\text{mean}} = 500$ MPa and $\sigma_a = 100$ MPa, batch 3.

The analysis of fracture surfaces yields the following picture. Fatigue cracks often initiate on casting defects in material interior. An example is shown in Fig. 3. The fracture surface corresponds to the specimen No. 5 from the batch 1 loaded in symmetrical cycle at the stress amplitude of 180 MPa. A large casting defect can be seen in the site of the crack initiation. The fracture surface appearance at low magnification and the circular crack front give evidence of internal crack propagation from the initiation site towards the specimen surface. Another observed type of fatigue crack initiation and propagation is shown in Fig. 5. Wide plane facets along $\{111\}$ crystallographic planes having mirror appearance at low magnification intersect individual grains. Macroscopically plain facets intersect shrinkage porosity and also larger casting defects. This is visible in Fig. 6. The dendrite structure, interdendritic regions and cut casting pores are well seen. No evidence of rubbing can be seen on the facets. Their appearance suggests decohesion of material along the $\{111\}$ crystallographic planes. Fig. 7 shows profiles of fracture surfaces of specimens from batches 1, 2 and 3 as observed on metallographically prepared axial sections. In all cases the loading was characterized by

high tensile mean stress. The number of cycles to fracture was in all cases of the order of 10^5 . Fracture profile on Fig. 7a corresponds to the specimen No. 67 (indicated in Fig. 2) prepared from the batch 1 loaded at $\sigma_{\text{mean}} = 600$ MPa and $\sigma_a = 130$ MPa. The arrow indicates plain crystallographic facets in the area of initiation of the fatigue crack, resulting in final fracture. Fig. 7b shows the fracture profile of the specimen No. 1 from the batch 2, loaded at $\sigma_{\text{mean}} = 500$ MPa and $\sigma_a = 70$ MPa. The crack initiation region is situated between the arrows. The crack started at large casting pore; the fracture surface in this region is formed directly by the surface of the casting defect. Moreover, the frequency of casting defects near the fracture surface is in the case of batch 2 substantially higher than that of batch 2 (Fig. 7a). The fracture profile connects many of them. The fracture surface profile of the specimen No. 82 from the batch 3 loaded at $\sigma_{\text{mean}} = 500$ MPa and $\sigma_a = 100$ MPa is presented in Fig. 7c. Analogous to the preceding case, the crack started at the casting pore.

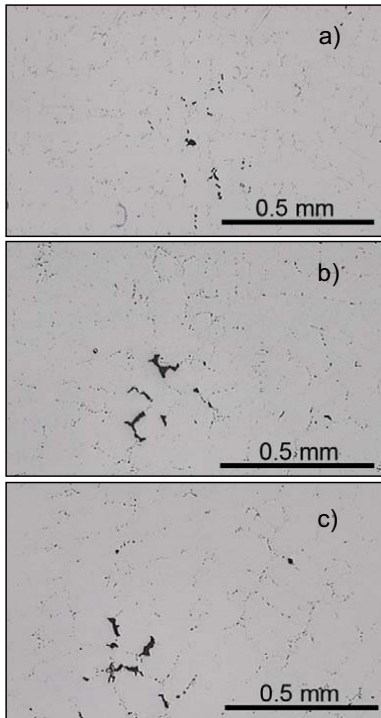


Fig. 8 Casting defects in specimen from a) batch 1, b) batch 2 and c) batch 3.

law fit is shown in Fig. 10. The upper and lower level of this interval for 10^7 cycles is 157 and 118 MPa, respectively.

Tensile mean stress results generally in lower fatigue strength in high-cycle fatigue region. Indeed, the experimental points in Fig. 2 are shifted towards lower lives with increasing mean stress. However, the effect is partly shielded by the large scatter of experimental data and also by the scatter of data corresponding to the particular batches. The problem is that even nominally identical batches prepared at the same casting conditions in engineering practice may exhibit differences in the size and distribution of casting defects. They are decisive factor reducing the fatigue life. This fact confirms fractographic observation of initiation of fatigue cracks on defects, often in material interior. From the practical engineering point of view it is important to stress that defect size, strongly influencing the lifetime, can be below the resolution limit of non-destructive defectoscopic methods.

Three examples of polished and metallographically prepared axial sections of material from batches 1, 2 and 3 are shown in Fig. 8. The casting defects in form of pores and shrinkages can be well seen. Gumbel probability plots, constructed on the basis of determination of the largest defect area for three batches studied are shown in Fig. 9. It is obvious from the figure that the maximum casting defect size notably differs for particular batches.

Discussion

Fig. 10 compares high-cycle fatigue data corresponding to fractured specimens obtained in this work with data published for IN 713LC loaded in low-cycle fatigue region [1]. It can be seen that power law can fit well all data in LCF and HCF regions, though there is a difference in conducting of fatigue tests in the discussed studies. Obrtlík and coworkers [1] performed the fatigue testing under fully reversed total strain cycle and the stress amplitudes were determined at half-life. The 95% confidence interval for the power

Statistical extreme value theory, introduced 50 years ago, has been used and further developed for determination of maximum inclusion size in very high strength steels by Murakami [8]. The method enables to estimate the maximum inclusion size likely to occur in large areas or volumes. Since that time the method has been applied for different materials, e.g. for evaluation of porosity in cast Al-Si alloy [9] or Al- and Mg- castings [10]. Also modification of this method was proposed to account for the simultaneous presence of different types of inclusions or defects [11].

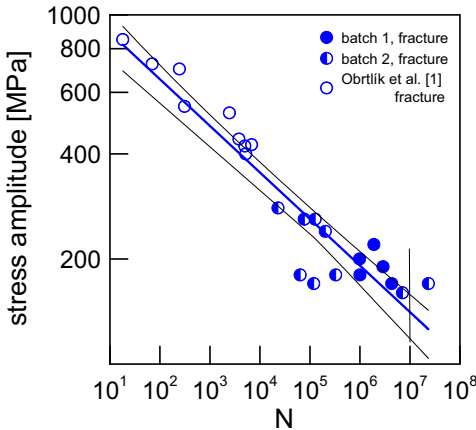


Fig. 9 Gumbel plot for three nominally identical batches of IN 713LC.

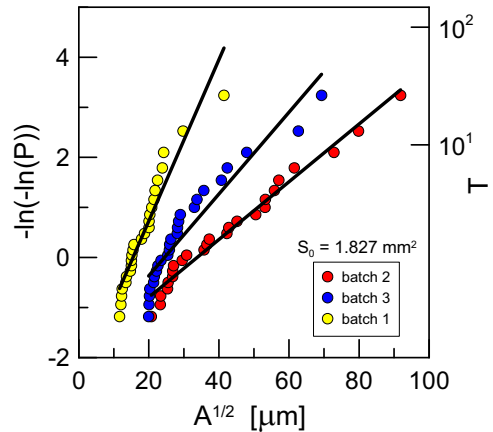


Fig. 10 S-N curve of IN 713LC with 95% confidence interval.

The three data sets of extreme values of casting pore size, $A^{1/2} \equiv \sqrt{area_{max}}$ determined by means of optical microscopy for three batches studied are shown in Fig. 9. The trend of the dependences is linear, which means that the casting defects follow the lognormal distribution. The Gumbel plot can be used for prediction of largest defect in given volume, using the return period T [8]. From the slope of three curves it follows that specimens manufactured from the batch 2 will contain larger maximum defects than specimens manufactured from batches 3 or 1. The batch 1 is from the point of view of maximum defects of the best quality. The largest expected casting defect size is in batch 2 three times larger than that in the material from the batch 1. The fatigue strength is in coincidence with this fact. The lifetime of specimens from the batch 1 is generally higher than that of batches 3 and 2. The plot in Fig. 9 enables to predict the maximum casting defect size in the axial section of the specimen. The return period T for the axial section of the whole gauge length is equal to 96, which yields the largest defect size of about $A^{1/2} = 110 \mu m$ for the batch 2 and $40 \mu m$ for the batch 1. These predicted values are small compared to the dimensions of casting defects observed at the fracture surfaces, e.g. in Fig. 3, where the defect of the total diameter of nearly 1 mm can be seen. The reason for this disagreement consists in the fact that the casting defects create clusters, Fig. 8. The evaluation by means of image analysis does not take this fact into account and counts only areas of individual pores. On the other hand, the crack initiation process involves the influence of defect clusters; the stress concentrations of individual defects in a cluster interfere and result in lower fatigue strength.

The experimentally observed large scatter of S-N data can be rationalized not only by the direct stress concentration effect of large pores on crack initiation and subsequent non-crystallographic crack propagation. In the case of crystallographic crack initiation and formation of large crystallographic facets the dimension of active planes is of the order of grain size, which is in cast IN 713LC several millimeters. The decohesion along this planes due to cycling proposed by Duquette et al. [7] results in formation of internal cracks which may substantially differ by size.

That is why the fatigue lifetime of particular specimens can vary substantially, according to the particular structural details.

Conclusions

The high-cycle fatigue life of cast IN 713LC alloy at 800 °C was experimentally determined for symmetrical loading cycle and for tensile mean stresses up to 600 MPa. The tensile mean stress results in shorter lifetime.

Casting defects cause considerable scatter of S-N data in high-cycle fatigue region. Two different types of crack initiation were observed. Initiation on large casting defects with subsequent non-crystallographic crack propagation and crystallographic initiation resulting in development of large crystallographic facets.

The application of the largest extreme value distribution method to statistical description of maximum equivalent casting defect differentiate among particular batches of otherwise nominally identical material. The qualitative evaluation is in agreement with the mutual relation of fatigue strength of individual batches. However, the troublesome fact in the prediction of the largest casting defects is the clustering of casting pores, which were not taken into account and which have to be treated to reach more reliable predictions.

Acknowledgements

This work was supported by the project FT/TA4/023, Ministry of Industry and Trade of the Czech Republic. This support is gratefully acknowledged.

References

- [1] K. Obrtlík, J. Man, J. Polák: In: Proc. of Euromat 2001 Conference, Rimini 2001, AIM Milano 2001.
- [2] N. Boutarek, D. Saïdi, M. A. Acheheb, M. Iggui, S. Bouteфраia: *Mater Charact* (2007), doi: 10.1016/j.matchar.2007.08.004.
- [3] M. Petre nec, K. Obrtlík, J. Polák, J.: *Mater. Sci. Eng. A* 400-401 (2005) p. 485.
- [4] Information on http://ec.europa.eu/research/transport/projects/article_6513_en.html.
- [5] P. N. Queded, S. Osgerby: *Mater. Sci. and Technol.* 2 (1986) p. 461.
- [6] M. J. Donachie and S. J. Donachie: *Superalloys. A Technical Guide*, 2nd Edition. ASM Int. 2002, p. 266.
- [7] D. J. Duquett, M. Gell, J. W. Pieto: *Met. Trans.* 1 (1970) p. 3107.
- [8] Y. Murakami: *Metal Fatigue: Effects of Small defects and Nonmetallic Inclusions*. Elsevier, 2002.
- [9] G. Nicoletto, R. Konečná, P. Biacchi, V. Majerová: *Material Science Forum* 567-568 (2008) p. 393.
- [10] M. Tiryakioğlu: *Mater. Sci. Eng. A* 476 (2008) p.174.
- [11] S. Bretta, C. Anderson, Y. Murakami: *Acta Mater.* 54 (2006) p. 2277.